A Structural Theory for Non-stoicheiometry. Part III.† Defect Fluorite-type Structures: Vacancy Superstructures in Ordered Praseodymium Oxides

By **Bernard F. Hoskins**, Department of Inorganic Chemistry, University of Melbourne, Parkville, Victoria, Australia 3052
Raymond L. Martin,* Research School of Chemistry, Australian National University, P.O. Box No. 4, Canberra, Australia 2600

The hypostoicheiometric composition region $MO_{2-\delta}$ ($0.286 \geqslant \delta \geqslant 0$) of binary lanthanoid oxides is re-examined in the light of new electron diffraction data on ordered praseodymium oxides Pr_nO_{2n-2} with $n = 7, 9, 10, 11$, and 12. Model structures have been devised which are consistent with the topological requirements of the co-ordination defect (c.d.) and the implications of the new unit-cell data. The metal-centred pairing of c.d.s along $[111]_F$, to yield the structural unit of composition $Pr_7O_{12}\square_2$, is a fundamental determinant in all phases. The vacancy sets for the triclinic homologues have been defined uniquely and those possible for the monoclinic phase β-$Pr_{12}O_{22}$ have been reduced to two alternatives. Planar ordering of anion vacancies characterizes both the triclinic (odd-n) and monoclinic (even-n) homologues. Possible inter-relations between their structures are analysed in terms of an extension of the crystallographic shear formalism.

THE detailed structural characterization of individual members of the binary fluorite-related non-stoicheiometric praseodymium oxides has remained an elusive problem of significance in understanding the nature of the defect solid state. *X*-Ray diffraction methods have been of limited value due, in part, to the practical difficulty of obtaining suitable homogeneous crystals of the desired composition. In addition, crystallographic twinning, coherent intergrowth between homologous phases, absorption errors, and large superstructures of low symmetry have all combined to make studies, even with single crystals, a formidable task.

In the previous papers,[1,2] an attempt was made to formulate structural principles from which model structures can be developed for individual members of the M_nO_{2n-2} fluorite-type non-stoicheiometric oxides. The basic premise requires that each vacant anion site in the *C*1 lattice remains co-ordinated by an octahedron of nearest oxygen neighbours to generate a 'co-ordination defect' or c.d. The composition of the c.d., $Pr_{3.5}\square O_6$, is that of the stable ι-phase and its distinctive topology reduces greatly the total number of potential anion sites upon which the oxygen deficiency of the lattice can be accommodated. By employing a matrix representation, superstructures of low symmetry (*e.g.* monoclinic or triclinic) can be readily visualized for the homologues by representing the structure in terms of the cubic *C*1 lattice.

The structure and composition of the stable ι-phase is determined uniquely by the close-packing of c.d.s which

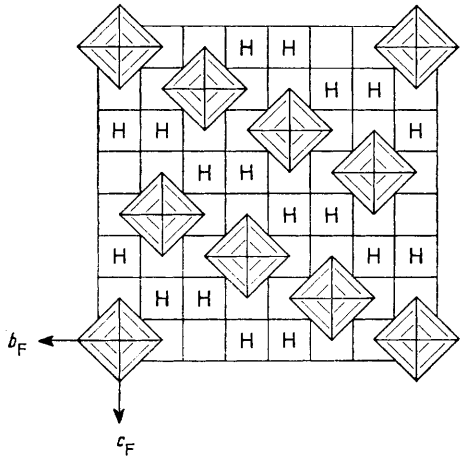

FIGURE 1 Idealized square-matrix representation of a $(100)_F$ layer of the fluorite (PrO_2) lattice showing the location of vacant oxygen sites in ι-Pr_7O_{12} along $[0\bar{2}1]_F$ (and $[0\bar{1}3]_F$) directions. Mating holes for accommodating contiguous layers are designated by H

can be described in terms of stacking successive $(100)_F$ layers of octants of the fluorite cube. In each $(100)_F$ layer the c.d.s are aligned in rows parallel to the $[0\bar{2}1]_F$ direction (Figure 1) but contiguous layers are displaced

† Part I, see ref. 1. Part II, see ref. 2.

[1] R. L. Martin, *J.C.S. Dalton*, 1974, 1335.
[2] B. F. Hoskins and R. L. Martin, *J.C.S. Dalton*, 1975, 576.

by the vector $\frac{1}{2}[1\bar{1}2]_F$ in order to ensure correct phasing of the metal lattice. As a result, c.d.s occur in rows along $[21\bar{1}]_F$ [Figure 2(a)] although the closest spacing between c.d.s, and their metal-centred pairing, is found in the $[111]_F$ direction [Figure 2(b)]. The greatest concentration of vacant oxygen sites occurs on $\{2\bar{3}1\}_F$ planes and, in the absence of structural information, it was suggested [1] that models for the more oxidized hypostoicheiometric homologues might likewise be based on regularly spaced $(2\bar{3}1)_F$ intergrowths of the progenitive ι- and PrO_2-phases.

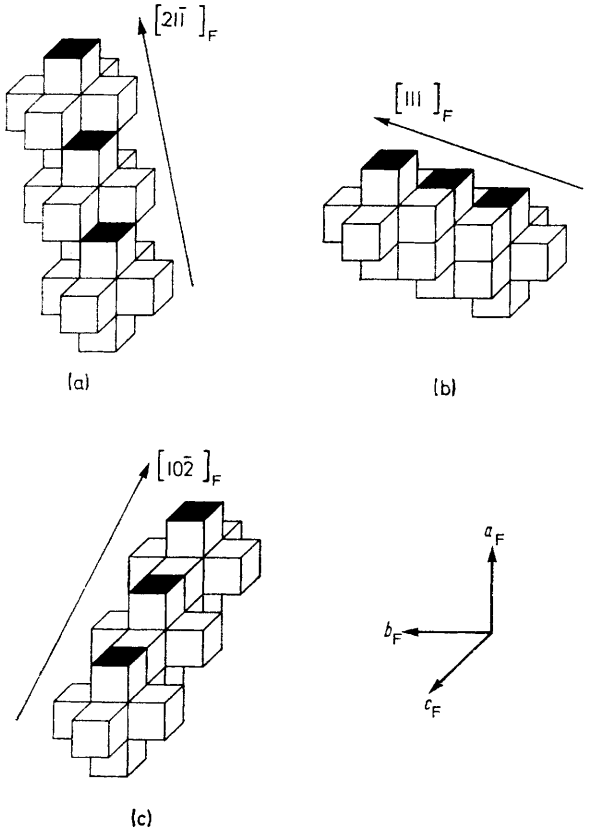

FIGURE 2 (a) A fragment of the ι-Pr_7O_{12} structure showing the arrangement of c.d.s. along the $[21\bar{1}]_F$ direction. (b) Arrangement of c.d.s. of the ι-Pr_7O_{12} phase in the $[111]_F$ direction showing the closest distance occurring between vacancy sites and the direction along which the metal-centred pairing occurs. (c) Arrangement of c.d.s. along $[10\bar{2}]_F$ direction

The results of *X*-ray single crystal [3] and electron diffraction [4] studies of β-$Pr_{12}O_{22}$ which subsequently became available, establish the dimensions of a superstructure with monoclinic symmetry. Although this monoclinic cell is not compatible with infinite rows of vacancies along either $[11\bar{1}]_F$ or $[0\bar{2}1]_F$ as in ι-Pr_7O_{12}, a topological analysis based on c.d.s suggested a structural model with edge dimensions and directions bearing an identical relationship to the *C*1 fluorite structure as do the axes of the observed monoclinic unit cell.[2] In this model the c.d.s were grouped in pairs, their centres being separated by $\frac{1}{2}[1\bar{1}1]_F$, and having the composition $Pr_7O_{12}\square_2$. The vacancy pairs were gathered on $(011)_F$ planes and lay along $[21\bar{1}]_F$ directions.

In a recent publication Kunzmann and Eyring [5] have succeeded in further defining the symmetry and unit cell parameters for each of the homologues with $n = 7$, 9, 10, 11, and 12 determined from electron diffraction patterns taken in a high-resolution transmission electron microscope from very small single crystals. The odd members are found to be differentiated from the even members of the series by possessing at least two, rather than one, axes of the $\frac{1}{2}[21\bar{1}]_F$ type, which is a structural element common to all the intermediate phases. Kunzmann and Eyring propose a formal structural relationship between the triclinic phases ι-Pr_7O_{12}, ζ-Pr_9O_{16}, and δ-$Pr_{11}O_{20}$, by hypothesising that all possess identical layers of vacancy pairs parallel to the *a*- and *c*-axes. Likewise, their suggestion that the monoclinic phases ε-$Pr_{10}O_{18}$ and β-$Pr_{12}O_{22}$ are built of identical layers of vacancy pairs perpendicular to the *b*-axis conforms in this respect to our model suggested in Part II. There are, however, several structures compatible with the unit cell data for the ε- and β-phases and unresolved ambiguities remain.

These new unit-cell data provide the necessary information for the structural ideas formulated in Part I to be evaluated. Although the symmetry and dimensions of the superlattices have now been determined, the exact location of oxygen vacancies cannot always be ascertained uniquely. Accordingly, it remains important to confirm whether structural predictions based on the topology of the co-ordination defect can aid both in devising, and minimizing the number of, trial structures required for elucidating data from *X*-ray, electron diffraction, and neutron profile [6,7] (Petten) methods. Using the data given by Kunzmann and Eyring, each Pr_nO_{2n-2} phase is considered below in terms of the topological requirements of the c.d. to determine whether detailed representations of the vacancy superstructures related to the *C*1 lattice can be developed. In addition, an attempt is made to define further the underlying structural inter-relationships, especially between the odd- and even-membered homologues.

(I) *The Odd Homologues*

The ι-Pr_7O_{12} *Phase.*—Structural studies [5,8] have shown that this ordered phase is isostructural with Tb_7O_{12},[9] $Zr_3Sc_4O_{12}$,[10] and $Zr_3Yb_4O_{12}$,[11] and isomorphous with

[3] M. Z. Lowenstein, L. Kihlborg, K. H. Lau, J. M. Hascke, and L. Eyring, Proc. 5th Materials Research Symposium, Nat. Bureau Standards Special Publ. No. 364, 1972, p. 343.
[4] L. Eyring and L. Tai, *Ann. Rev. Phys. Chem.*, 1973, **24**, 189.
[5] P. Kunzmann and L. Eyring, *J. Solid State Chem.*, 1975, **14**, 229.
[6] B. O. Loopstra and H. M. Rietveld, *Acta Cryst.*, 1969, **B25**, 787.
[7] H. M. Rietveld, *J. Appl. Cryst.*, 1969, **2**, 65.
[8] R. B. Von Dreele, L. Eyring, A. L. Bowman and J. L. Yarnell, *Acta Cryst.*, 1975, **B31**, 971.
[9] N. C. Baenziger, H. A. Eick, H. S. Schuldt, and L. Eyring, *J. Amer. Chem. Soc.*, 1961, **83**, 2219.
[10] M. R. Thornber, D. J. M. Bevan, and J. Graham, *Acta Cryst.*, 1968, **B24**, 1183.
[11] M. R. Thornber and D. J. M. Bevan, *J. Solid State Chem.*, 1970, **1**, 536.

Bartram's phases ULu_6O_{12} and UY_6O_{12}.[12] These possess a rhombohedral cell, space group $R\bar{3}$, with two vacant oxygen sites per unit cell which are situated along the rhombohedral three-fold axis of symmetry. The three axes of the rhombohedral cell are related to the parent fluorite lattice according to the transformations:

$$a_1 = a_F + \tfrac{1}{2}b_F - \tfrac{1}{2}c_F$$
$$a_2 = -\tfrac{1}{2}a_F + b_F + \tfrac{1}{2}c_F$$
$$a_3 = \tfrac{1}{2}a_F - \tfrac{1}{2}b_F + c_F$$

and the structure can be described readily in terms of the fluorite sub-lattice using the c.d. concept. The distribution of c.d.s in each $(100)_F$ octant layer of the ι-phase is shown in Figure 1, the axes being chosen to conform with the cubic orientations of Kunzmann and Eyring. The mating holes (H) are required to satisfy the topological requirements of the c.d.s of the contiguous $(100)_F$ layers. Since each point defect along $[0\bar{1}\bar{3}]_F$ is related to another by the vector $\frac{1}{2}[21\bar{1}]_F$, the acancies aranion ve gathered as metal-centred pairs on $(2\bar{3}1)_F$ planes and lie in strings along the $[111]_F$ direction (see Figure 6, Part I). The faces of the rhombohedral cell are comprised of $\{1\bar{5}\bar{3}\}_F$ planes and the arrangement of the vacant oxygen sites on a single $(1\bar{5}\bar{3})_F$ plane is illustrated in Figure 3 together with the rhombohedral

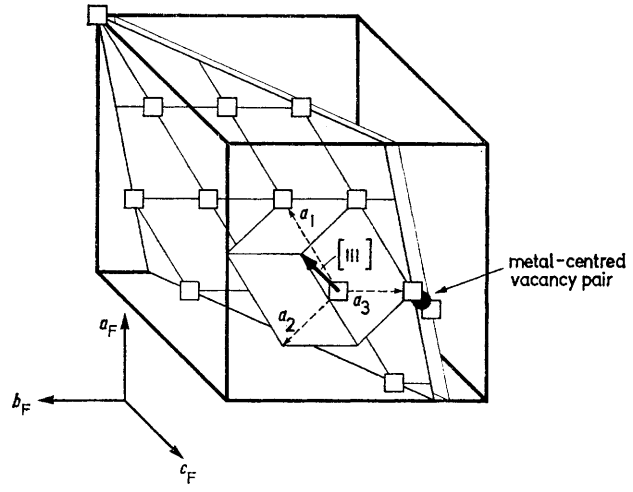

FIGURE 3 Isometric projection of idealized cubic cell ($7d \times 7d \times 7d$) for ι-Pr_7O_{12} showing the distribution of vacant anion sites on a vacancy-only $(1\bar{5}\bar{3})_F$ plane. The outlined rhombohedral cell shows the $[111]_F$ direction. A metal-centred vacancy pair which forms in the $[111]_F$ direction from a contiguous vacancy-only $(1\bar{5}\bar{3})_F$ plane is delineated

unit cell of the ι-phase outlined on the basis of the vacant anion sites. The formation, from an adjoining $(1\bar{5}\bar{3})_F$ plane, of a metal-centred pair of c.d.s along $[111]_F$, which has the chemical composition $Pr_7O_{12}\square_2$, is also delineated in Figure 3. It is now known that apart from the terminal member C-Pr_2O_3, ι-Pr_7O_{12} seems to be the only one of the known binary phases to possess vacancy pairs aligned in strings in the $[111]_F$ direction. As well as the $[111]_F$ relationship, each metal-centred pair of c.d.s is operated on by the three translation vectors of the type $\frac{1}{2}[21\bar{1}]_F$ that define the unit-cell axes. The orientation of the $\frac{1}{2}[111]_F$, $\frac{1}{2}[10\bar{2}]_F$, and $\frac{1}{2}[21\bar{1}]_F$ vectors (*cf.* Figure 2) possessed by two metal-centred pairs of c.d.s in the ι-phase appears to be important and common to all the higher homologues. A cluster of four c.d.s showing these vector relationships is illustrated in Figure 4 (*cf.* Figure 2).

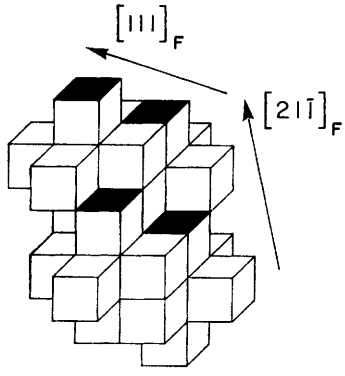

FIGURE 4 A cluster of two metal-centred pairs of c.d.s. of the ι-Pr_7O_{12} phase showing the important vector orientations which are believed to be common to all the higher Pr_nO_{2n-2} homologues

The ζ-Pr_9O_{16} *Phase.*—The unit cell of the ζ-phase is triclinic and the structure can be related formally to the parent fluorite lattice *via* the transformations,

$$a = a_F + \tfrac{1}{2}b_F - \tfrac{1}{2}c_F$$
$$b = \tfrac{3}{2}b_F + \tfrac{1}{2}c_F$$
$$c = \tfrac{1}{2}a_F - \tfrac{1}{2}b_F + c_F$$

Kunzmann and Eyring have noted that the a and c axes of ζ have the same orientational relationship to two of the three axes of ι, so that the two structures have one plane in common and differ only in the length and orientation of the third axis. Employing the reasonable hypothesis that the arrangement of vacancies along the $[21\bar{1}]_F$ and $[1\bar{1}2]_F$ directions should always be the same, they have proposed that planes of metal-centred $[111]_F$ related vacancy pairs parallel to the a and c axes, having the same two-dimensionally periodic structure of ι, are stacked together with the distance and orientation appropriate to the b-axis. If this hypothesis is correct, then the structure is defined unambiguously and can be readily described in terms of the c.d. concept by employing a single $(100)_F$ octant layer of the structure. It is clear from the cell transformation that all $(100)_F$ octant layers have an identical arrangement of c.d.s in that the adjacent layers are displaced by the vector $\frac{1}{2}[1\bar{1}2]_F$, which corresponds to the c-axis of the superstructure. Figure 5(a) shows the pattern of c.d.s in a typical $(100)_F$ layer. Again, H is used to denote the mating holes necessary to accommodate the topological requirements of the c.d.s between contiguous layers. The crystallographic triclinic unit cell of the ζ-phase

[12] S. F. Bartram, *Inorg. Chem.*, 1966, **5**, 749.

showing the $(1\bar{5}\bar{3})_F$ orientation of the *ac*-plane is illustrated in Figure 5(b).

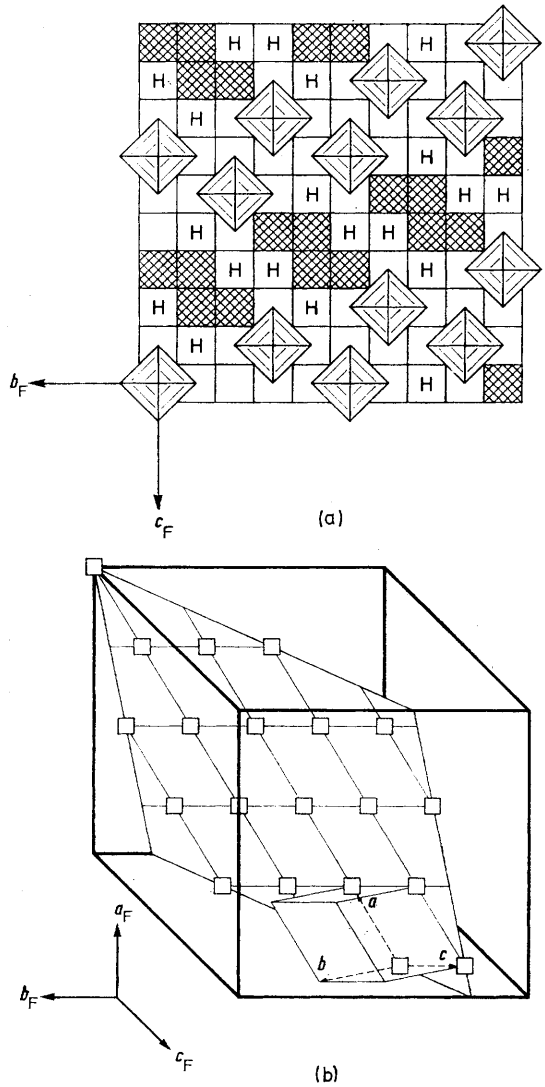

FIGURE 5 (a) The pattern of c.d.s in a typical $(100)_F$ octant layer of the ζ-Pr_9O_{16} structure. The adjacent layer is displaced by the vector $\frac{1}{2}[1\bar{1}2]_F$. (b) Isometric projection of idealized cubic cell ($9d \times 9d \times 9d$) for the ζ-Pr_9O_{16} phase showing the $(1\bar{5}\bar{3})_F$ orientation of an *a-c* vacancy-only plane and the triclinic unit cell

This model is one of the two only possible structures compatible with the topological requirements of the c.d. and the unit-cell data. The other model gives an arrangement of c.d.s such that the vacant oxygen sites lie on $(2\bar{1}3)_F$ planes and in strings along $[1\bar{1}\bar{1}]_F$, *i.e.* a structure identical to that shown in Figure 8(b) of Part I. It is known that Pr_9O_{16} can exhibit two polymorphic modifications, one being rhombohedral at higher temperatures and the other triclinic at lower temperatures. It is possible that the model suggested in Part I, which involves strings of vacancies along $[1\bar{1}\bar{1}]_F$, is the rhombohedral modification of this phase.

The δ-$Pr_{11}O_{20}$ *Phase.*—The more oxidized δ-phase is also triclinic with a and c dimensions equal to ι and ζ but differing in the length and orientation of the b-axis. The primitive triclinic unit cell is related to the basic fluorite lattice by the vectors:

$$a = a_F + \tfrac{1}{2}b_F - \tfrac{1}{2}c_F$$
$$b = -\tfrac{1}{2}a_F + \tfrac{3}{2}b_F + c_F$$
$$c = \tfrac{1}{2}a_F - \tfrac{1}{2}b_F + c_F$$

The combination of unit-cell data and the orientation of the vacancy pairs anticipated from the relationship of this phase to ι defines uniquely the anion vacancy sites of the δ-phase. From the unit cell data it is clear that

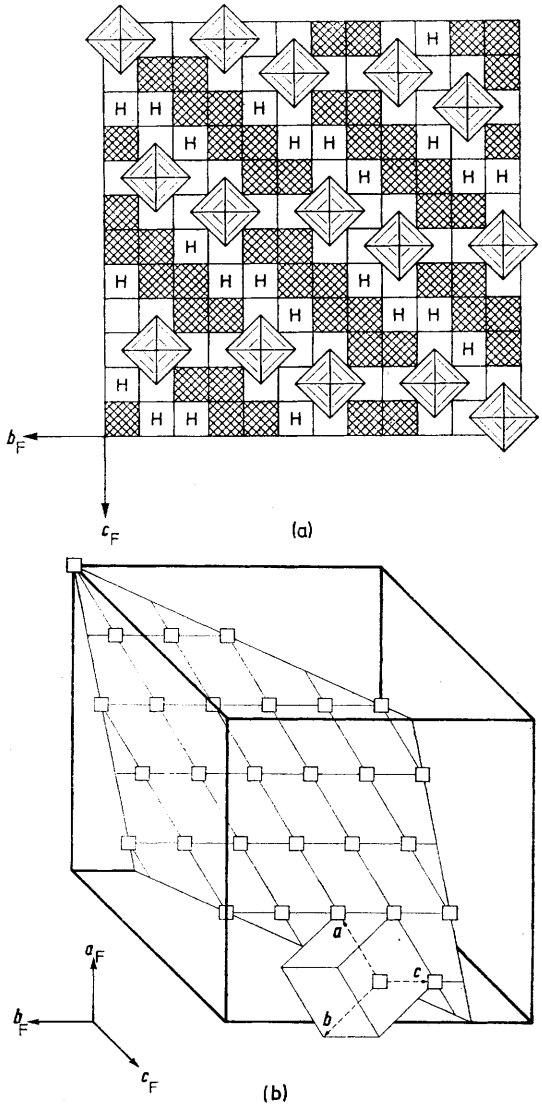

FIGURE 6 (a) The distribution of c.d.s in a $(100)_F$ octant layer of δ-$Pr_{11}O_{20}$. Adjacent layers are displaced by the vector $\frac{1}{2}[1\bar{1}2]_F$. (b) Isometric projection of idealized cubic cell ($11d \times 11d \times 11d$) for δ-$Pr_{11}O_{20}$ showing the $(1\bar{5}\bar{3})_F$ orientation of the *a-c* vacancy-only plane and the triclinic unit cell

each $(100)_F$ octant layer has exactly the same distribution of c.d.s which is shown in Figure 6(a). Adjacent

layers are displaced by the vector $\frac{1}{2}[1\bar{1}2]_F$ (or $\frac{1}{2}[\bar{1}32]_F$) and H again is used to denote the necessary mating holes. The crystallographic triclinic unit cell of the δ-phase showing the $(1\bar{5}\bar{3})_F$ orientation of the *ac*-plane is illustrated in Figure 6(b).

A systematic topological analysis reveals only two other structures compatible with the topology of the c.d. and the unit-cell characteristics. One model leads to a structure involving isolated anion vacancies, rather than pairs, distributed throughout the lattice. The second structure, however, does involve vacancy pairs but in the alternative orientation, $[1\bar{1}\bar{1}]_F$. These alternative models provide indications of possible polymorphism in $Pr_{11}O_{20}$.

(II) *The Even Homologues*

X-Ray diffraction data on single crystals of an ordered phase were first reported [3] for β-$Pr_{12}O_{22}$, which established a fluorite-type sub-lattice with a superstructure of monoclinic symmetry. Since the intensities of the superstructure reflections were dominated by small shifts of the metal atoms and because the large absorption errors could not be corrected because of twinning, attempts by these authors [3] to determine the arrangement of oxygen vacancies were unsuccessful.

The new data [5] establish that the other even homologue ε-$Pr_{10}O_{18}$ is also monoclinic and that both phases retain just one of the unit-cell vectors characteristic of the ι-phase. Kunzmann and Eyring suggest that the ε- and β-phases are composed of identical layers perpendicular to *b* since both possess a common plane which is defined by their *a*- and *c*-axes and is parallel to a glide plane.

The arrangements of vacant oxygen sites which comply with the superstructure lattice parameters for the even members is considered below in terms of the topology of the co-ordination defect.

The β-$Pr_{12}O_{22}$ *Phase.*—The basic characteristics of the β-phase which comply with *X*-ray single-crystal data [3] were described [2] in Part II. The new high-resolution electron-diffraction data [5] confirm the relationship of the superstructure unit-cell parameters to the basic structure unit-cell parameters is:

$$a = a_F + \tfrac{1}{2}b_F - \tfrac{1}{2}c_F$$
$$b = \tfrac{3}{2}b_F + \tfrac{3}{2}c_F$$
$$c = -2b_F + 2c_F$$

In addition, the space group *Pn* necessitates two differing vacancy pair orientations. Taking this into account, a systematic topological analysis reveals only two possible non-equivalent models if the vector $\frac{1}{2}[21\bar{1}]_F$ is assumed to indicate an arrangement and orientation of vacancy pairs along the *a*-axis which is the same as in ι. If the corners of the unit cell are defined by the metal atoms of metal-centred $[111]_F$ related pairs of c.d.s, each of the two unique models is generated by positioning the glide plane at either *b*/12 or 3*b*/12; the other possible glide-plane positions lead to structures equivalent to one or other of these. The three adjacent $(100)_F$ layers necessary to define each structure are shown in Figures 7 and 8. Structures for the β-phase are generated in three-dimensions by stacking the structural units outlined in Figures 7 and 8 up the a_F axis.

Each model will be seen to have two different vacancy pair orientations ($[111]_F$ and $[1\bar{1}\bar{1}]_F$) which are contained on the $(0\bar{1}1)_F$ planes. The arrangement of c.d.s in a cluster of two metal-centred vacancy pairs, each having

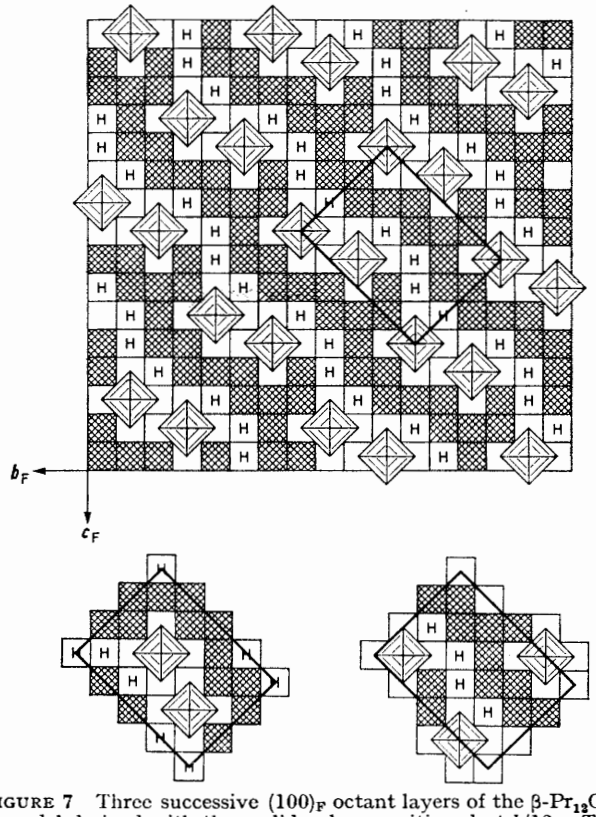

FIGURE 7 Three successive $(100)_F$ octant layers of the β-$Pr_{12}O_{22}$ model derived with the *n*-glide plane positioned at *b*/12. The three-dimensional arrangement is obtained by stacking the units of structure shown for each layer along the $[100]_F$ direction

the $[1\bar{1}\bar{1}]_F$ orientation, is shown in Figure 9. This bears a mirror-image relationship across the $(011)_F$ plane to the fragment of the ι structure shown in Figure 4. Two $(0\bar{1}1)_F$ planes, showing the direction of the *b*-axis and the two orientations of metal-centred c.d.s, is illustrated in Figure 10(a).

An $(011)_F$ plane of this structure, showing the directions of the *a* and *c* axes, is illustrated in Figure 10(b).

It seems particularly significant in terms of the unknown Pr_8O_{14} phase that each of the models proposed for β possesses a sequence of $(011)_F$ planes such that there are four of composition $Pr_8O_{14}\square_2$ to two of Pr_8O_{16}. This will be discussed further in a later section.

The ε-$Pr_{10}O_{18}$ *Phase.*—The ε-phase is monoclinic with

space group Pn and is related to the fluorite lattice by the transformations:

$$a = a_F + \tfrac{1}{2}b_F - \tfrac{1}{2}c_F$$
$$b = \tfrac{5}{2}b_F + \tfrac{5}{2}c_F$$
$$c = -2b_F + 2c_F$$

In order to define the structure of this phase, it is necessary to establish the relative positions of two

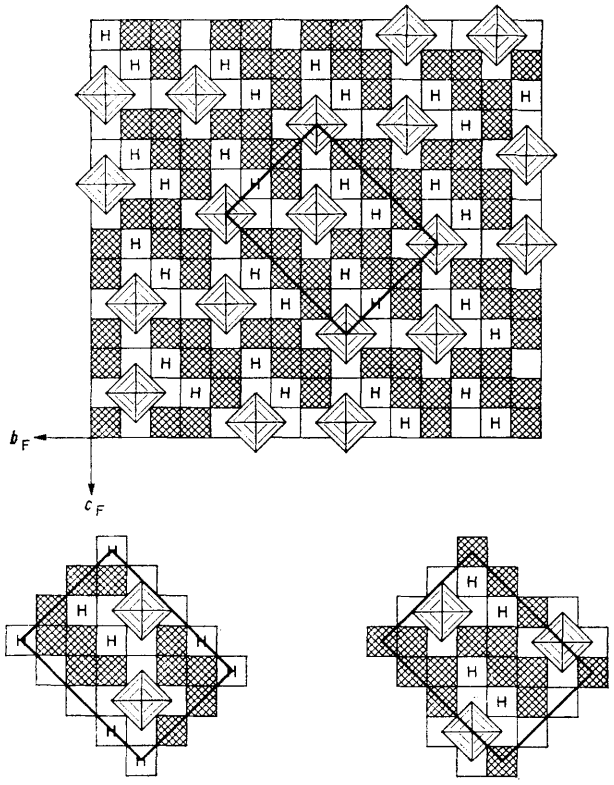

FIGURE 8 The three $(100)_F$ octant layers which define the β-$Pr_{12}O_{22}$ model based on an n-glide plane at $3b/12$. The three-dimensional arrangement is obtained in the same manner as that for the model shown in Figure 7

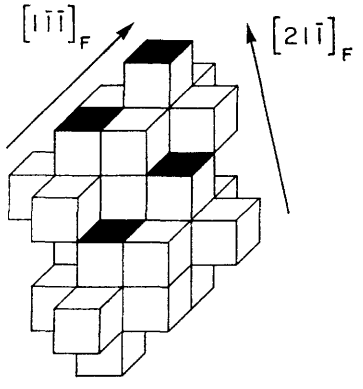

FIGURE 9 The vector arrangement possessed by the cluster of c.d.s obtained by the reflection of that shown in Figure 4 across an $(011)_F$ plane. The two different vacancy pair orientations depicted in Figures 4 and 9 are found in the monoclinic even homologues

metal-centred vacancy pairs and the n-glide plane. There are a number of models possible for ε-$Pr_{10}O_{18}$ but

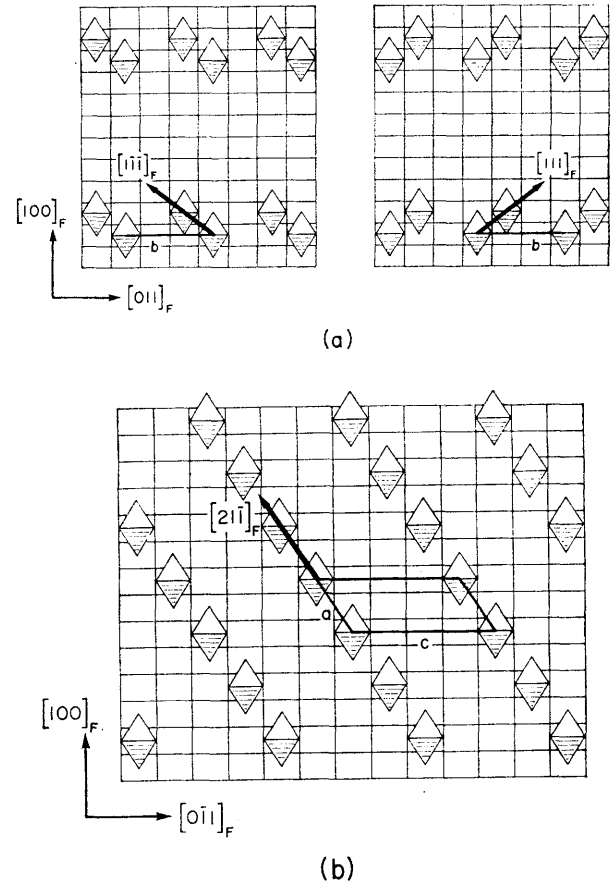

FIGURE 10 (a) Two $(0\bar{1}1)_F$ planes of the structure proposed for β-$Pr_{12}O_{22}$ showing the monoclinic b-axis and the alternative orientations of metal-centred c.d.s. (b) An $(011)_F$ plane of this structure showing the monoclinic a and c axes

the presence of a $\frac{1}{2}[21\bar{1}]_F$ vector for this homologue again inclines us to the same arrangement and orientation of vacancy pairs along the a-axis as occurs in ι-Pr_7O_{12}. The glide plane indicates that the two different vacancy pair orientations again exist in this structure. The $\frac{1}{2}[21\bar{1}]_F$ relationship indicates that this structure too involves $(011)_F$ planes of composition $Pr_8O_{14}\square_2$. One of several models consistent with the Pn space group, and the c.d. orientations suggested by the unit cell dimensions is illustrated in Figure 11.

The Unknown Phase Pr_8O_{14}.—One of the more unusual features of the ordered non-stoicheiometric oxides in this region is the apparent absence of the member $n = 8$. Ternary lanthanoid oxides of this composition frequently possess the cubic pyrochlor ($E8_1$) structure in which the anion vacancies are also octahedrally coordinated by oxygen atoms (*cf.* Figure 15 of Part I). It is interesting, and we believe significant, that some of the $(011)_F$ planes of both the β- and ε-phases have the composition $Pr_8O_{14}\square_2$ as a consequence of the $\frac{1}{2}[21\bar{1}]_F$ relationship between metal-centred vacancy pairs. This

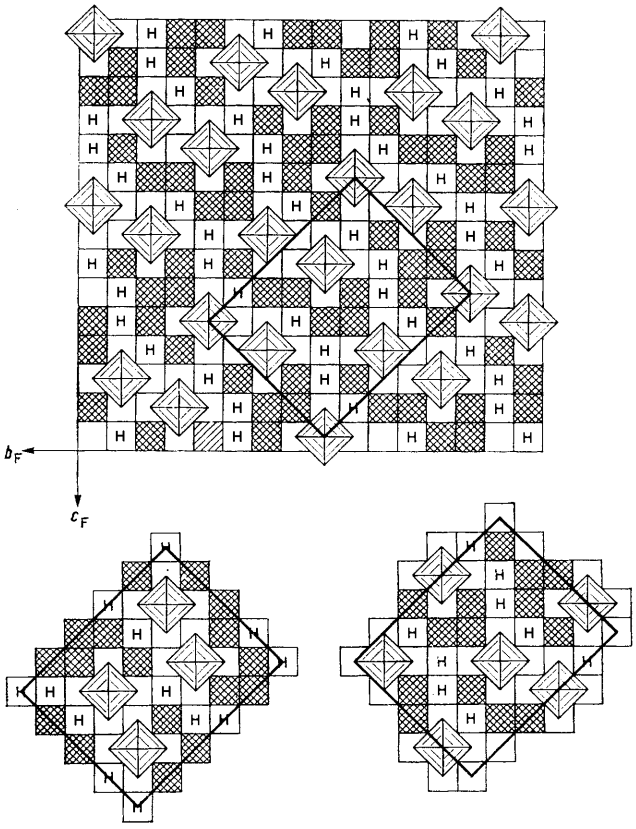

FIGURE 11 One possible model for ε-$Pr_{10}O_{18}$, having the expected vector orientations between the metal-centred pairs of c.d.s, which is consistent with the unit cell dimensions and the *Pn* space group

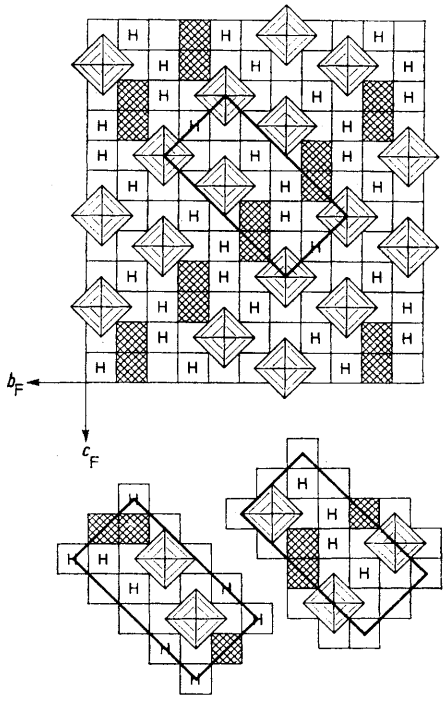

FIGURE 12 Three successive $(100)_F$ octant layers of the conjectural monoclinic phase Pr_8O_{14}. The three-dimensional arrangement is obtained as for the β-$Pr_{12}O_{22}$ structure shown in Figure 7

suggests a possible structure for a phase of composition $Pr_8O_{14}\square_2$. The unit cell of this conjectural monoclinic Pr_8O_{14}-phase containing two anion vacancies is illustrated in Figure 12 which is related to fluorite *via* the transformations:

$$a = a_F + \tfrac{1}{2}b_F - \tfrac{1}{2}c_F$$
$$b = \tfrac{1}{2}b_F + \tfrac{1}{2}c_F$$
$$c = -2b_F + 2c_F$$

There appears to be no obvious structural feature which might preclude the independent existence of this ordered homologue.

(III) *Crystallographic Shear in the Hypostoicheiometric Region*

In Part II, a structural model for the hyperstoicheiometric region $MO_{1.500+\delta}$ $(0 \leqslant \delta \leqslant 0.214)$ was developed by the formal procedure of deleting progressively $(2\bar{3}1)_F$ oxygen-intact planes from the ι-lattice and then restoring the lattice by a crystallographic shear (c.s.) mechanism. The possibility of applying conventional c.s. concepts to an oxygen-centred lattice is an advantage consequent on the integrity of octahedral $\square O_6$-c.d.s being preserved in the hyperstoicheiometric fluorite region.

It emerges from the preceding discussion that the new unit-cell information for praseodymium oxides in the hypostoicheiometric region $MO_{2-\delta}$ $(0.286 \geqslant \delta \geqslant 0)$ can also be reproduced by structural models developed from the concept that all vacant anion sites remain octahedrally co-ordinated by oxygen atoms. It is instructive then to ascertain whether these phases (*i.e.* $n = 7$—12 in Pr_nO_{2n-2}) can likewise be inter-related through the formal process of crystallographic shear.

In the model proposed in Part I, hypostoicheiometric PrO_x phases were generated through the formalism of progressive incorporation of additional $(2\bar{3}1)_F$ planes of composition PrO_2 into the type ι-Pr_7O_{12} lattice. However, the new information on unit-cell symmetries and dimensions, reveals that the alternative and less-densely populated oblique plane $(1\bar{5}\bar{3})_F$ is actually the preferred plane for the odd-membered oxidized homologues ζ-Pr_9O_{16} and δ-$Pr_{11}O_{20}$. The relationship between these phases and the parent ι-Pr_7O_{12} phase can be represented formally in terms of a crystallographic shear in the $[0\bar{1}1]_F$ direction along the trace of $(1\bar{5}\bar{3})_F$ on an $(100)_F$ plane. Since $[0\bar{1}1]_F$ shear operations conform to the metal-atom phasing, the cation lattice can be regarded as being invariant to the shear operations of this type performed on the anion lattice. The procedure can be conveniently visualized by employing the Anderson and Hyde 'scissor' method [13,14] whereby a drawing of an $(100)_F$ octant layer of ι-Pr_7O_{12} is cut along the line $[0\bar{3}5]_F$ in which oxygen sites are to be created [*cf.* Figure 13(a)] and then opened up by the $\frac{1}{2}[0\bar{1}1]_F$ shear to effect

[13] J. S. Anderson and B. G. Hyde, *Bull. Soc. chim. France*, 1965, 1215.

[14] J. S. Anderson and B. G. Hyde, *J. Phys. and Chem. Solids*, 1967, **28**, 1393.

the insertion of oxygen. For example, the production of an unoccupied $(1\bar{5}\bar{3})_F$ anion plane characteristic of Pr_nO_{2n-2} is illustrated in Figure 13(b) and this corresponds to the formation of a $(1\bar{5}\bar{3})_F$ sheet of Pr_8O_{14} inserted coherently into the parent ι-Pr_7O_{12} matrix. The structural unit in $(100)_F$ outlined in black in Figure 13(b) can be stacked along a to give a triclinic unit cell structural element of the triclinic phases; however, only in Pr_8O_{14} [Figure 13(b)] and $Pr_{12}O_{22}$ [Figure 13(f)] can an axis of the $[011]_F$ type be discerned which is common to the observed monoclinic polymorphs for $n = 10$ and 12. This suggests that the structural features of the odd-membered are quite closely related to those of the even-membered phases.

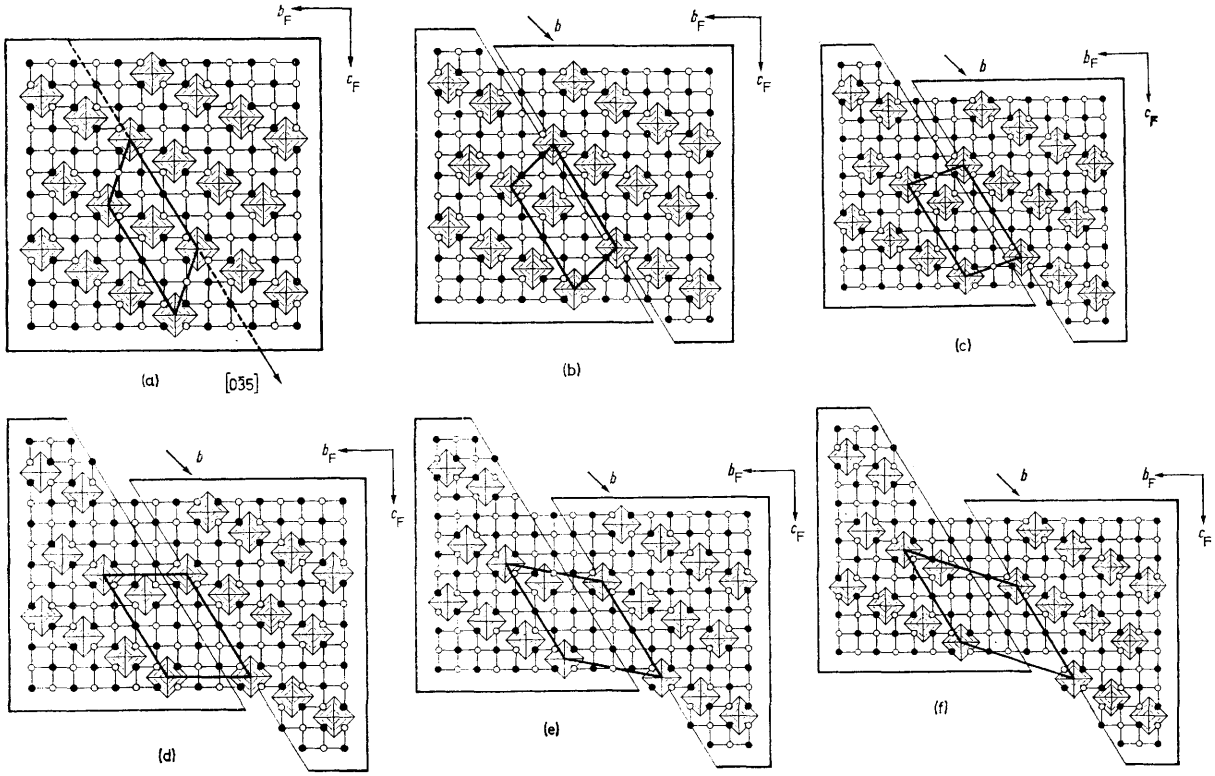

FIGURE 13 (a) An idealized $(100)_F$ structural octant layer of ι-Pr_7O_{12} showing the line in the $[0\bar{3}5]_F$ direction along which oxygen sites will be created using the shear operation $\frac{1}{2}[0\bar{1}\bar{1}]_F$. The metal atoms can be regarded as invariant. (b) Formation of $(1\bar{5}\bar{3})\frac{a}{2}[0\bar{1}1]_F$ shear plane corresponding to the production of a $(1\bar{5}\bar{3})_F$ sheet of composition Pr_8O_{14} inserted coherently into the parent ι-Pr_7O_{12} matrix (b = Burgers vector). (c) The formation of a $(100)_F$ octant layer of the ζ-Pr_9O_{16} phase by the incorporation of two additional $(1\bar{5}\bar{3})_F$ anion planes into ι-Pr_7O_{12} using the c.s. procedure above. (d) Conjectural triclinic modification of $Pr_{10}O_{18}$. (e) δ-$Pr_{11}O_{20}$; observed structural repeat unit outlined in black. (*f*) Conjectural triclinic modification of $Pr_{12}O_{22}$

which preserves the $\frac{1}{2}[21\bar{1}]_F$ and $\frac{1}{2}[1\bar{1}2]_F$ vectors for the a- and c-axes, respectively. The b-axis lies along $[011]_F$ and the superstructure contains two oxygen vacancies per unit cell. The vacancies are grouped into metal-centred pairs along $[111]_F$ and are located in $(1\bar{5}\bar{3})_F$ planes as illustrated in Figures 3, 5(b), and 6(b).

The known triclinic unit cells of the ζ-Pr_9O_{16} and δ-$Pr_{11}O_{20}$ phases [*cf.* Figures 5(a) and 6(a)] are reproduced likewise by the systematic incorporation of two and four additional $(1\bar{5}\bar{3})_F$ planes of oxygen atoms into the ι-Pr_7O_{12} matrix by the crystallographic shear operation [*cf.* Figures 13(c) and 13(e)] followed by the appropriate stacking of the $(100)_F$ octant layers to preserve the $\frac{1}{2}[21\bar{1}]_F$ and $\frac{1}{2}[1\bar{1}2]_F$ vectors.

The unknown triclinic polymorphs of Pr_8O_{14}, ε-$Pr_{10}O_{18}$, and β-$Pr_{12}O_{22}$, derived by this c.s. procedure are depicted in Figures 13(b), 13(d), and 13(f). The $(100)_F$ units all possess the $\frac{1}{2}[0\bar{3}\bar{5}]_F$ axis which is a common

This close relationship can be illustrated by considering the transformation of the hypothetical triclinic polymorph of $Pr_{12}O_{22}$ to the monoclinic β-phase. This may be depicted, for a single $(100)_F$ layer of octants, as the series of co-operative jumps $(a_F/\sqrt{2})$ along $[011]_F$ between oxygen anions and vacant sites illustrated in Figure 14; *i.e.*,

$$\square/an + O^{2-}/an \rightleftharpoons O^{2-}/an + \square/an \qquad (1)$$

Since oxygen sites are not eliminated, the composition but not the symmetry of the homologue remains unchanged. Furthermore, since the oxygen-vacancy interchanges occur along the $[011]_F$ direction, the triclinic ⇌ monoclinic transformation may be envisaged in terms of introducing an antiphase boundary (a.p.b.) by crystallographic shear along $[011]_F$ with the shear vector being in a parallel direction (*cf.* Figure 15). This formalism was implicit in earlier discussions [2] of the

transformations of type $D \longrightarrow$ type C-Pr_2O_3 [*cf.* Figure 6(b), Part II]. Unfortunately, since the contiguous $(100)_F$ layers of the β-phase are inter-related by

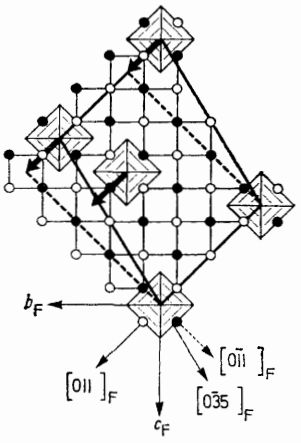

FIGURE 14 Transformation of conjectural triclinic $Pr_{12}O_{22}$ structure $\longrightarrow$ monoclinic β-$Pr_{12}O_{22}$ *via* the series of concerted oxygen $\rightleftharpoons$ vacancy switches of $\frac{1}{2}[011]_F$ in a $(100)_F$ layer

the *n*-glide symmetry operation (*cf.* Figure 7), an a.p.b. plane cannot be defined; *i.e.*, a.p.b. operations of the type illustrated in Figure 15 must be applied individually to each successive $(100)_F$ layer.

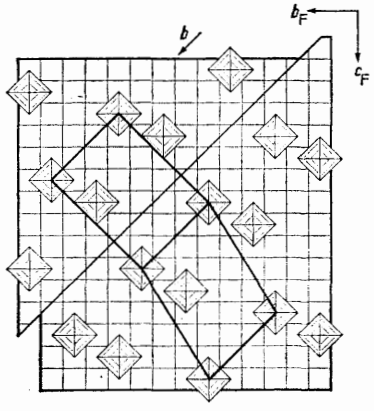

FIGURE 15 Formation of anti-phase boundary (a.p.b.) in a $(100)_F$ layer of the conjectural triclinic modification of $Pr_{12}O_{22}$. Structural units of the triclinic and monoclinic polymorphs are delineated

(IV) *Conclusions*

The recent refinement of the crystal structure of Pr_7O_{12} by powder neutron diffraction and the new electron-diffraction data on the ordered phases with $n = 7$, 9, 10, 11, and 12 has enabled the distribution of anion vacancies in a fluorite lattice to be defined in reasonable detail. Although some uncertainties and ambiguities remain unresolved, the principles upon which the superstructures are based are beginning to emerge.

The ι-phase is of central significance and its structural element, the co-ordination defect $Pr_{3.5}\square O_6$, together with octants of the fluorite cube, $Pr_{0.5}O$, form the basis of all the more oxidized ordered phases. The evidence that the c.d.s occur in metal-centred pairs of composition $Pr_7\square_2O_{12}$ is convincing and the structures of UY_6O_{12} and Pr_7O_{12} suggest that the metal atom of higher oxidation state (*i.e.* smaller radius) displays a preference for sites with six co-ordination. Defect clusters comprising two paired c.d.s of overall composition $Pr_{14}\square_4O_{24}$ can be discerned in all the homologues. These create a $\frac{1}{2}[21\bar{1}]_F$ axis in the superstructures and involve c.d.s paired along $[111]_F$ in the triclinic phases, and along both $[111]_F$ and $[1\bar{1}\bar{1}]_F$ in the monoclinic phases. Essentially the unit cells of all the oxidized homologues are constituted from these defect clusters of ι contained in a matrix of fluorite-type PrO_2. The defect clusters themselves are aggregated into columns of ι along the $[21\bar{1}]_F$ direction, each containing a core of six-co-ordinated cations.

The nature of the progression from the present ordered phases with fully defined superstructures to the more disordered non-stoicheiometric phases, such as α-PrO_x which overlays the hypostoicheiometric composition region, remains unknown. However, the transition, order $\rightleftharpoons$ disorder, now appears likely to involve the sequential disruption of columnar units, of defect clusters, and finally dissociation of metal-centred paired co-ordination defects; *viz.*,

$$[Pr_7\square_2O_{12}]_{2\infty} \text{ columns} \rightleftharpoons \infty[Pr_7\square_2O_{12}]_2 \text{ defect clusters} \quad (2)$$

$$[Pr_7\square_2O_{12}]_2 \text{ defect clusters} \rightleftharpoons 2[Pr_7\square_2O_{12}] \text{ paired c.d.s} \quad (3)$$

$$[Pr_7\square_2O_{12}] \text{ paired c.d.s} \rightleftharpoons 2[Pr_{3.5}\square O_6] \text{ isolated c.d.} \quad (4)$$

Evidence for the dissociation of metal-centred paired c.d.s, equation (4), may prove difficult to obtain since the characterization of an isolated c.d. in the α-phase requires the resolution of metal atoms which are seven-co-ordinate randomly distributed in a disordered matrix of eight-co-ordinated cations. However, the ordered phases δ′-$TbO_{1.809}$ ($n = 10\frac{1}{3}$)[5] and $Zr_{48}Sc_{14}O_{117}$ [15] may offer a more promising prospect for achieving this objective.

Finally, the planar ordering of anion vacancies in the region $PrO_{1.5}$–$PrO_{2.0}$ deserves brief comment. The anion deficiency of the stable ι-phase can be described as being accommodated by point defects which are gathered, either at a maximum density on $(2\bar{3}1)_F$ planes or at a lower density on $(1\bar{5}\bar{3})_F$ planes. The electron-diffraction data establish that the triclinic oxidized phases are based on regularly spaced $(1\bar{5}\bar{3})_F$ intergrowths of the progenitors ι-Pr_7O_{12} and PrO_2. These phases may be generated then through the formalism of progressive incorporation of additional $(1\bar{5}\bar{3})_F$ planes of composition PrO_2 into the ι-Pr_7O_{12} lattice rather than

[15] M. R. Thornber, D. J. M. Bevan, and E. Summerville, *J. Solid State Chem.*, 1970, **1**, 545.

involving the alternative $(2\bar{3}1)_F$ planes postulated previously.[1] In contradistinction, the known structures of the reduced phases (C-M_2O_3 and the ternary oxides Sr_2UO_5 and Cd_2UO_5) appear to require the systematic elimination of $(2\bar{3}1)_F$ rather than $(1\bar{5}\bar{3})_F$ planes from ι-Pr_7O_{12} to rationalize the superstructures of the reduced oxides.[2] Thus the ι-phase, which is unique in possessing both $(2\bar{3}1)_F$ and $(1\bar{5}\bar{3})_F$ vacancy planes, enjoys a pivotal relationship to the more reduced and the more oxidized ordered phases. We believe that this is a reflection of the structural rôle played by the co-ordination defect.

[5/1817 *Received, 22nd September,* 1975]